Nonlinear Soil–Structure Interaction: Foundation Uplifting and Soil Yielding

George Gazetas[(1)] and Marios Apostolou[(2)]

The study investigates the response of shallow foundations subjected to strong earthquake shaking. Nonlinear soil–foundation effects associated with large deformations due to base uplifting and soil failure are examined in comparison with the conventional linear approach. Soil behavior is represented with the elastoplastic Mohr-Coulomb model. The interplay between foundation uplifting and soil failure of the bearing capacity type is elucidated under static and dynamic conditions.

Keywords**:** *shallow footing, soil–foundation interaction, uplift, bearing capacity, soil failure*

1. INTRODUCTION

Research on seismic soil–foundation interaction in the last three decades has mostly relied on the assumption of linear (or at most equivalent-linear) viscoelastic soil behavior and fully–bonded contact between foundation and soil. Seismic design of structure foundation systems has followed a somewhat parallel path : the still prevailing "capacity design" philosophy allows substantial plastic deformation in the superstructure but requires that no significant "plastification" should take place below the ground level. This means that :

- foundation elements must remain structurally elastic (or nearly elastic)
- bearing–capacity soil failure mechanisms must not be mobilized
- sliding at the soil–foundation interface must not take place, while the amount of uplifting must be restricted to about ½ of the total contact area.

However, seismic accelerograms recorded in the last twenty years, especially during the Northridge 1994 and Kobe 1995 earthquakes, have shown that very substantial ground and spectral acceleration levels can be experienced in the near–fault zones. Seismic loads transmitted onto shallow foundations in such cases will most probably induce significant nonlinear inelastic action in the soil and soil–foundation interface. Figure 1 illustrates the three possible types of foundation–soil nonlinearity.

Observations in past earthquakes confirm the above argument. The most dramatic examples of bearing–capacity and uplifting failures of building foundations took place in the city of Adapazari, during the Kocaeli 1999 earthquake. But such phenomena are not limited to buildings : as an example of a modern monumental bridge, we mention the Rion–Antirrion cable–stayed bridge, the surface foundations of which, despite their colossal 90 m diameter, had to be designed allowing for sliding, uplifting and partial mobilization of soil rupture mechanisms to resist the prescribed high levels of seismic excitation (Pecker & Teyssandier 1998, Gazetas 2001).

[(1)] Professor, National Technical University, Athens, Greece
[(2)] PhD Candidate, National Technical University, Athens, Greece

Finally, for seismically retrofitting structures that had been designed with the small acceleration levels of the past, the necessity to explicitly consider the occurrence of one or more of the above nonlinearities is often unavoidable.

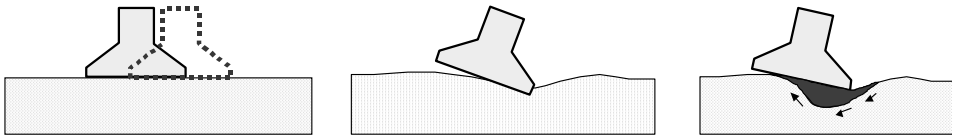

Sliding at the soil-foundation interface | **Foundation uplifting from the supporting soil** | **Bearing capacity type of soil failure**

Figure 1 Three types of nonlinearity in soil–foundation interaction

The present study investigates the interplay between the two (geometric and material) nonlinearities :

- separation of the rotationally oscillating footing from the supporting soil *("uplifting"),* and
- mobilization of bearing–capacity type failure surface mechanisms under large cyclic overturning moments *("soil failure").*

One of the aims is to show that under seismic excitation even when the minimum (with respect to time) factor of safety (against "uplifting" or "soil failure") is well below unity, structure and foundation response may be quite satisfactory. We begin by separating the occurrence of "uplifting" from "soil failure" and even from mere "soil yielding" : we study in the time domain the rocking response of a rigid block in tensionless contact with an elastic halfspace (homogeneous or layered). Although this idealized case would be directly applicable only to footings on very stiff ("non-yielding") soil, it serves as a basis for understanding the dynamics of the inelastic SSI system.

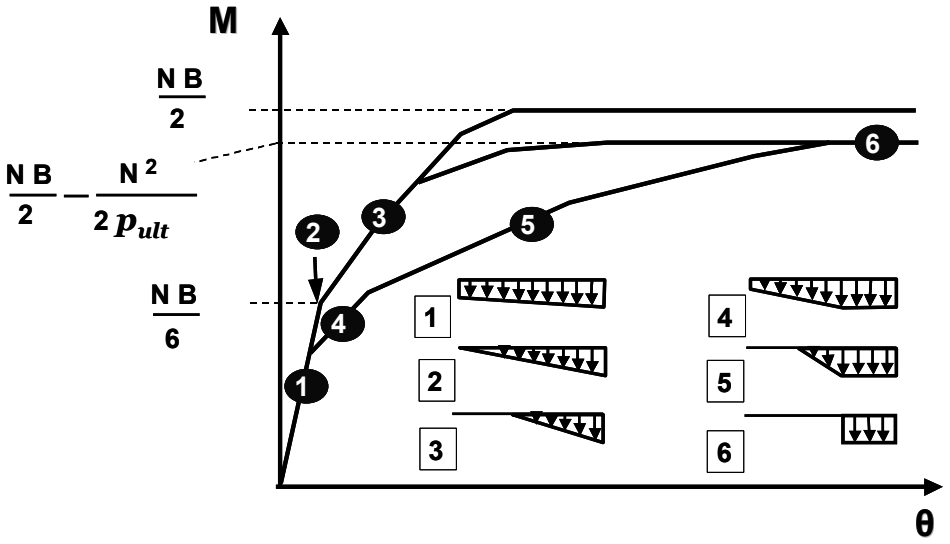

Figure 2 Idealization of the overturning moment–rotation response based on conventional Winkler modeling (Bartlet 1979)

Until recently, the only preferred model to account for soil reactions on a rigid strip footing was the Winkler elastoplastic model, according to which the foundation is assumed to rotate about its center even when large angles of rotation are imposed (Allotey & Naggar, 2003, Bartlett,1979). With the Winkler model there are two possible modes of response (illustrated in Fig 2) depending on whether the safety of factor for central vertical loading is greater or less than 2. For low values of vertical loading (FS < 2) uplift occurs at $M = N B / 6$ (point 2) before any soil yielding initiates. In this case the moment–rotation response follows the path (1)-(2)-(3)-(6). When FS > 2, soil yielding occurs when the entire base area is still in contact with soil , and the moment loading path is (1)-(4)-(5)-(6).

2. UPLIFTING AND OVERTURNING ON A VISCO-ELASTIC SOIL

Consider a foundation supported on a visco-elastic homogeneous half-space, with soil Young's modulus E_s and damping ratio ξ. Compared to the rocking response of a structure on perfectly rigid base, the compliance of supporting soil introduces additional degrees of freedom. The structure can now sustain rotational motion (without uplifting) for amplitudes of rotation below the critical value. The (geometrically) nonlinear nature of the problem is evident even under the assumption of an elastic soil.

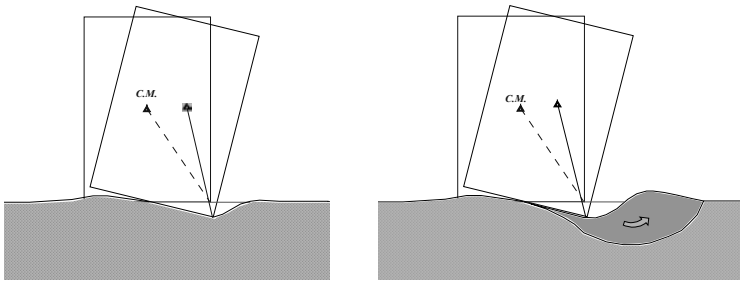

(a) Rocking on elastic, deformable soil **(b) Rocking on yielding soil**

Figure 3 The two rocking problems studied in the paper

Several analytical studies have already been published investigating the effect of soil compliance on rocking response of structures with foundation uplift. In these early studies (Psycharis, 1983, Chopra & Yim, 1985, Koh et al, 1986) the underlying soil was represented by distributed tensionless spring-dashpot elements. Recently, Crèmer & Pecker (2002) also analysed a foundation on inelastic continuum and developed a constitutive law to represent the uplift mechanics in an elastic or elasto-plastic soil through a single macro-element. In the present study the dynamic analysis of the rocking response is implemented with a finite element discretization using Abaqus (Hibbitt et al, 2001). The structure and the underlying soil are represented with plane-strain elements. An advanced contact algorithm has been adapted to incorporate potential slipping or uplifting of the foundation. For practical purposes the supporting soil is modelled as a homogeneous halfspace using 2D infinite elements.

We consider first a rigid rectangular structure with base width $B = 2\ m$ and height $H = 10\ m$ (aspect ratio $H / B = 5$) subjected to a base acceleration of $a = 0.30\ g$. Under static conditions the moment capacity of the foundation before it overturns is :

$$M_{ult} = N B / 2 \qquad (1)$$

where N is the permanent vertical load. (The load eccentricity e corresponding to this moment is of course equal to the foundation half-width, B/2.) The maximum induced overturning moment arising from the inertial force is:

$$M_{\max} = N \ (\alpha / g) \ H/2 \tag{2}$$

where a is the peak ground acceleration. For the above-mentioned structure $M_{ult} \approx 490\ kN$ and $M_{max} = 735\ kN$, and therefore

$$M_{max} = 1.5\ M_{ult} \tag{3}$$

In static terms, such an exceedance of the (ultimate) moment capacity of the foundation would have led to toppling of the structure (factor of safety 1/1.5 = 0.60). This is not the case however under dynamic loading: the foundation can sustain rocking motion safely even for values of the moment much higher than M_{ult}. The reason: the short duration (usually a small fraction of a second) that the exceedance of the moment capacity lasts. After the uplift has started and the body is on the way to toppling, a reversal of ground acceleration makes the block decelerate, stop, and start rocking in the opposite direction. Since the natural period of a rocking block at incipient failure can be quite large, such a reversal in rocking is very likely to occur, especially with high-frequency excitation. In other words, the more "dynamic" the ground shaking the easier for a rocking structure to survive!

This paradoxical phenomenon is illuminated for the aforementioned block subjected to two different ground motions: (a) the accelerogram of Düzce (EW component, $a = 0.37\ g$) recorded in the Izmit 1999 Earthquake, and (b) an idealized approximation in the form of the "Ricker wavelet", with $a = 0.30\ g$ and dominant period $T_E = 1.3\ sec$.

The angular displacement of the rocking foundation is computed initially for stiff supporting soil with Young's modulus $E_s = 100\ MPa$ and the results are plotted in Fig 4a in terms of rotation–angle time-histories. Evidently, despite the fact that $M_{max} = 1.50\ M_{ult}$, the structure undergoes rocking motion without toppling, with a maximum angle of rotation of about 0.08 *rad*, which is substantially lower than the critical angle for overturning under static conditions: $\theta_c = \arctan(B / H) \cong 0.2\ rad$. Furthermore, the two plots for the angle $\theta = \theta(t)$ are nearly identical, demonstrating : (i) that the simple pulse–type motion of a Ricker wavelet approximates remarkably well the essence of the Düzce accelerogram, and (ii) that the high–frequency spikes of the Düzce accelerogram do not affect the rocking response of the structure.

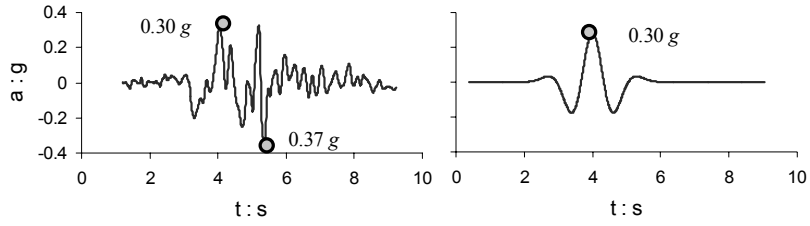

Figure 4. (a) The record of Düzce ($a = 0.37\ g$) from the 17–8–99 Izmit earthquake and (b) the Ricker wavelet pulse with $a = 0.3\ g$ and $T_E = 1.3\ sec$.

To investigate the effect of soil compliance on rocking response, the computed maximum angle of rotation, is plotted in Fig 4b for a range of E_s values (5 *MPa* – 1000 *MPa)*. For very high values of the modulus of elasticity, the amplitudes of rotation converge to the limiting case of the amplitude on rigid base ($\theta_{rigid} = 0.032\ rad$). Decreasing E_s the effect of soil deformability leads understandably to greater values of the maximum angle, which can go up

to $2^1/_2$ times the rigid base value. For even smaller values of E_s, less than about 10-15 *MPa,* the increased softening of the soil is beneficial, leading to smaller θ values! In all these cases (E_s > *5 MPa*), the structure oscillates in rocking without overturning, despite the pseudo-statically–predicted toppling. However, for very small values of E_s, less than about 2 to 5 *MPa*, the trend changes again and θ increases with decreasing E_s. Failure is now possible.

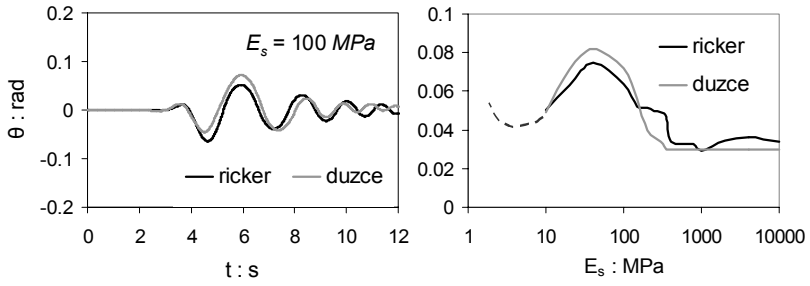

Figure 5 (a) Time-histories of rotation of a rectangular block–type structure with base width B = 2 *m* and height H =10 *m* on stiff elastic half-space, (b) Peak amplitude of the angle of rotation as a function of soil Young's models. (The critical angle for overturning under static conditions is about 0.2 *rad*, which is far greater than the maximum computed angle for all values of E_s, despite the "instantaneous" factor of safety of only 0.60.)

A parametric study is now carried out with smaller–size structures. A quite interesting rocking behavior is revealed as shown in Fig 6. Two more blocks are taken into consideration with base width 1.4 m and 1.0 m, and height 7.0 m and 5.0 m, respectively, so that, the aspect ratio is the same, H / B = 5, and thereby the critical angle of rotation remains also constant. In this example, it is the dimensions of each block, described through the half-diameter $R = [(B/2)^2 + (H/2)^2]^{1/2}$, that change (from 2.5 to 5.1 *m*).

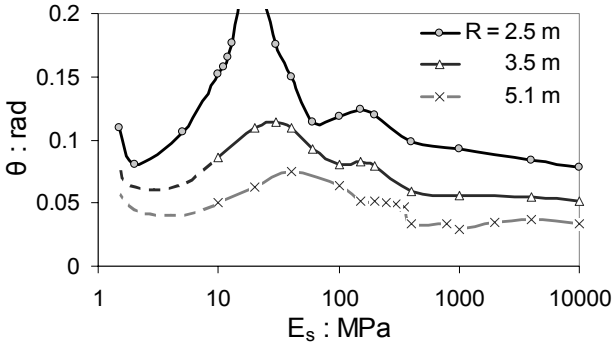

Figure 6 The peak amplitude of rotation of three rectangular block–type structures with constant aspect ratio H/B = 5 (equal critical overturning angle θ_c = 0.2 *rad)* . Excitation : Ricker 0.30 *g* and T_E = 1.3 *sec*.

The following trends are worthy of note in this figure :

1) the overall size of the block affects strongly its rotation ; the smallest of the three blocks undergoes the largest rotation for all values of E_s and it in fact overturns for E_s ~ 15 MPa.

2) the variation of θ_{max} with E_s is not monotonic ; it exhibits a peak at $E_s \approx$ 15 MPa – 30 MPa depending on block size, and again tends to become very large as $E_s \rightarrow 0$. A secondary peak is also noticed at $E_s \approx$ 150 MPa – 200 MPa. Nevertheless, the maximum rocking angle in case of soft soil would in most cases be not more than 1.5 to 2 times the corresponding "rigid-foundation" value.

The effect of soil stiffness on rocking and especially on the overturning potential can be further illustrated using sinusoidal pulse type excitations. In Fig 7 we consider the smallest of the three studied rectangular blocks, which has a base width of 1.0 *m* and a height of 5.0 *m* (hence, $H / B = 5$, $\theta_c \approx 0.2$ *rad,* and $R = 2.5$ *m*) resting on a visco–elastic halfspace.

Under a one-cycle sinusoidal excitation of period $T_E = 0.8$ *s* uplifting on rigid base initiates when the ground acceleration exceeds the critical value ($\alpha_c = 0.20$ *g*), but the structure overturns (after one impact in the opposite direction) only when *a* has increased up to $\alpha_{over} = 0.42$ *g*. However, for a soft soil, with Young's modulus $E_s = 10$ *MPa* the block rocks with uplifting but it does not overturn at $\alpha = 0.42$ *g*. The time history of the response reveals the secret of the success : thanks to its compliance, soil deforms due to moment loading in the first cycle of motion, leading to a much larger rotation *($\theta \approx 0.07$ rad)* of the block than the rotation *($\theta \approx 0.02$ rad)* on a rigid base. The next cycle is fatal for the block on rigid base (see the enlarged Fig 7b). For the block on soft soil, however, this strong-excitation cycle is consumed in first "arresting" the rotation towards the other side and, then, reversing the relatively large rotation (0.07 *rad*) ! Thus, it cannot make it to induce but a mere $\theta_{max} \approx 0.12$ *rad*, which is only 60% of the required θ_c for overturning. In fact, α must increase to 0.84 g (doubling the previous amplitude) for overturning to occur. Eventually, if we keep increasing α until it reaches and exceeds 1 g, the block overturns after the very first impact.

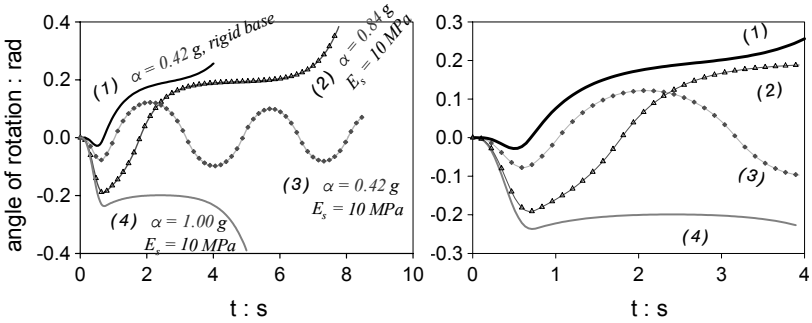

Figure 7 The time histories of rotation of a slender rigid block with $B = 1$ *m* and $H = 5$ *m* (critical angle $\theta_c \approx 0.2$ *rad* and $R = 2.5$ *m*), supported on elastic soil with E_s as an independent parameter. The excitation is a one-cycle sinusoidal pulse with period $T_E = 0.8$ *s* but with different peak acceleration for each curve. (The right figure is merely an enlargement of the first 4 seconds of motion shown on the left figure.)

To further demonstrate that the role of soil compliance in overturning of a rigid block can range from very *detrimental* to very *beneficial,* we present Figure 8, which needs no further explanation.

3. BEARING–CAPACITY FAILURE ENVELOPE UNDER LARGE SHEAR FORCE AND OVERTURNING MOMENT

An important intermediate step in the proposed method of soil-foundation interaction analysis is the computation for a given vertical (axial) load N, of the combination of the limiting values of shear force Q and overturning moment M that will create a failure mechanism in the soil under the foundation. The problem is 3–dimensional in nature, and recent research (Butterfield 1994, Bransby & Randolph 1998, Taiebat & Carter 2000) has shown that, for any foundation shape and supporting soil, there is a surface, in load space (N, Q, M) independent of loading path, containing all combinations of N, Q, and M that cause failure. This surface defines a bearing–capacity failure envelope for the foundation–soil system.

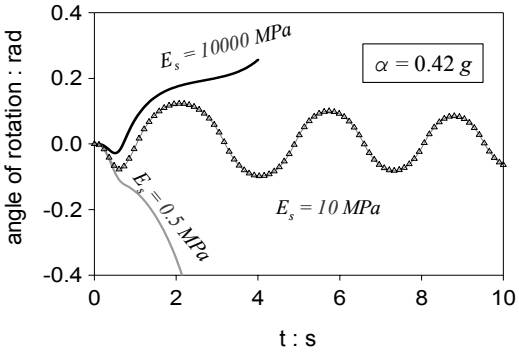

Figure 8 The time-histories of rotation of a slender rigid block with B = 1 *m* and H = 5 *m* (corresponding to a critical angle θ_c = 0.2 *rad* and R = 2.5 *m*), on elastic soil with E_s *as* the independent parameter. The excitation is a one-cycle sinusoidal pulse with period T_E = 0.8 *s* and constant peak acceleration, a = 0.42 *g*

While for relatively simple soil geometries such a the homogeneous halfspace limit analysis methods have provided closed-form expressions for the bearing–capacity *failure envelope*, for the general case of a layered profile comprising cohesive and cohesionless soils the finite element method has proved a versatile tool (e.g., Taiebat & Carter 2000).

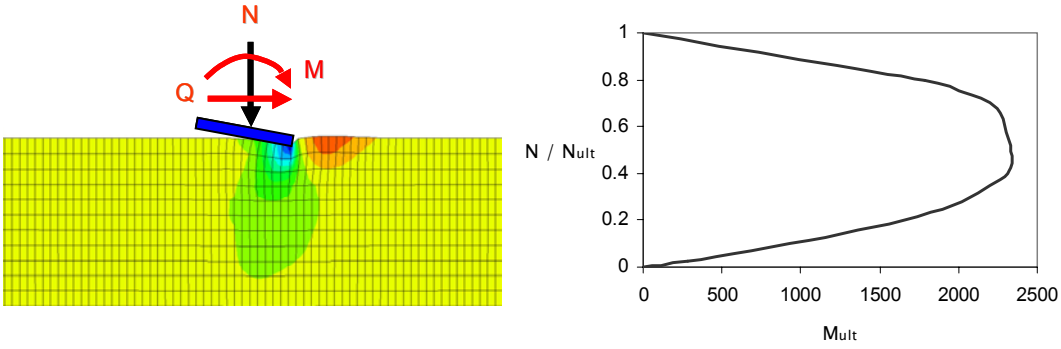

Figure 9 Plastic deformations at imminent failure of a 6 m wide strip foundation, and cross–section of the 3–dimensional bearing capacity failure envelope. (Min kNm/unit length.)

An example of a bearing capacity failure envelop for a strip foundation on a homogeneous soil is given in Fig 9, in which the top figure portrays the contours of plastic deformations developing under the uplifted foundation, while the bottom figure plots a cross–section of the failure envelope perpendicular to the shear–force axis (Q). Note that the maximum M_{ult} occurs when the vertical load is slightly less than ½ of the ultimate vertical capacity N_{ult} ; the Winkler model predicts exactly ½ .

4. NONLINEAR MOMENT–ROTATION RELATIONSHIP

The response of a strip shallow footing under static and dynamic loading is computed numerically with a plane–strain, finite element modeling. The footing is modeled with solid non-deformable 2-D elements. The soil is represented with solid elements and the horizontal boundaries with infinite elements. Nonlinear soil behavior is modeled with the elastoplastic M-C behavior, described by the limit state parameters c and φ. The superstructure is

approached with a lumped mass at the mass center, which is connected with the footing by a rigid and massless beam, so the inertia loading can be transmitted to the structural foundation. An advanced contact algorithm with gap elements has been implemented to model the interface between soil and foundation incorporating seperation–uplifting.

The system we study possesses two significant degrees of freedom, namely:

- Rotation of the base about axis y (clockwise is positive)
- Vertical displacement of the base center (upward is positive)

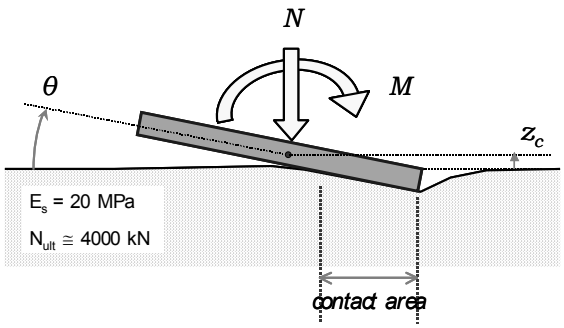

Figure 10 Configuration of the soil-foundation system examined in this study

Response under Static Loading : An Example

We consider a 6 m wide, rigid strip footing, which rests on a homogenous soil layer and is initially subjected only to vertical load N = 1000 kN (per unit of length). The ultimate vertical capacity, N_{ult}, is 4000 kN (per unit of length), i.e. the factor of safety against static bearing capacity failure is 4 – a lightly loaded foundation. The mass of the superstructure is assumed to be concentrated at a point 12 m over the base. The parameters affecting the soil-structure system are summarized in Table 1.

A displacement-controlled force is applied at the mass centre of the structure, resulting in a horizontal and moment loading of the footing. The applied displacement is gradually increased until toppling of the structure occurs.

Table 1 System parameters

Soil		**Foundation**	
Elastoplastic soil stratum over rigid bedrock		Rigid, strip footing	
Young modulus	20 MPa	Base width	6 m
M-C parameters	c = 50 kPa φ = 30°	Height of mass center	12 m
Ultimate vertical load (per unit of length)	4000 kN	Weight (per unit of length)	1000 kN
Layer depth	20 m	Flexibility of the superstructure	Negligible

Initially, the overturning moment increases linearly with rotation angle. However, uplifting and soil yielding initiation leads to a gradually softening rocking behavior and therefore, the moment of the footing reaches a maximum value of about 1900 kNm/unit length. This value is considerably lower than the 'elastic' expected moment capacity M = N B/2 = 3000 kNm and slightly lower than the maximum 'elastoplastic' moment (≅ 2250 kNm – see Fig 9). This additional reduction of the ultimate moment arises from the geometrically–induced nonlinearity of the problem.

By further increasing the imposed displacement, the overturning moment enters the declining region due to considerably increasing P–δ effects and eventually it reaches zero at the point of marginal overturning. The complete moment–rotation monotonic curve is plotted in Fig 11 and contrasted with the curve corresponding to an infinity stiff and strong (undeformable) soil.

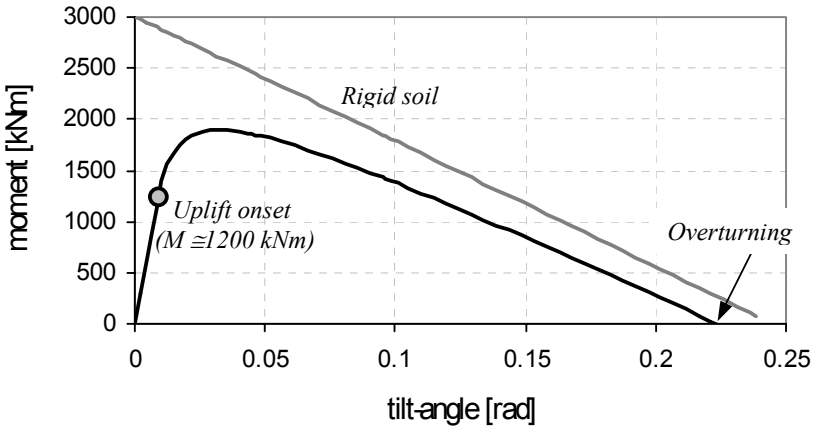

Figure 11 Moment-rotation monotonic curve

We repeat the above procedure for parametrically varying values of the vertical load N. A quite impressive behavior is revealed: Initially when N is increased from $N = 0.25N_{ult} = 1000$ kN to $N \approx 0.42N_{ult} \approx 1700$ kN, the increased static settlement of the foundation delays the initiation of uplifting and leads to a higher value of maximum moment $M_{ult} \approx 2250$ kNm – the highest that can be achieved with any value of N (Fig 12). At this level of loading, the best possible combination of uplifting and soil plastification is achieved. This approximately an agrees with the conclusion of Bartlet (1979) and Allotey et al (2003). However, the descending branch of the M– θ curve drops faster, and hence the ultimate rotation at incipient overturning is slightly reduced from 0.22 rad for $N = 1000$ kN to 0.20 rad for $N = 1700$ kN.

As the applied vertical load is further increased beyond N = 1900 kN/m the maximum moment starts decreasing, as a result of the increased rate of plastification. The ultimate rotation angle at incipient overturning continues to decrease.

A parabolic M–N interaction diagram for the footing (a cross–section of the failure envelope) is plotted in Fig 13. The maximum moment capacity of the footing occurs when the vertical load is at or a little less than half the bearing capacity load of the supporting soil, namely at a static factor of safety of the order of 2 to 2.5.

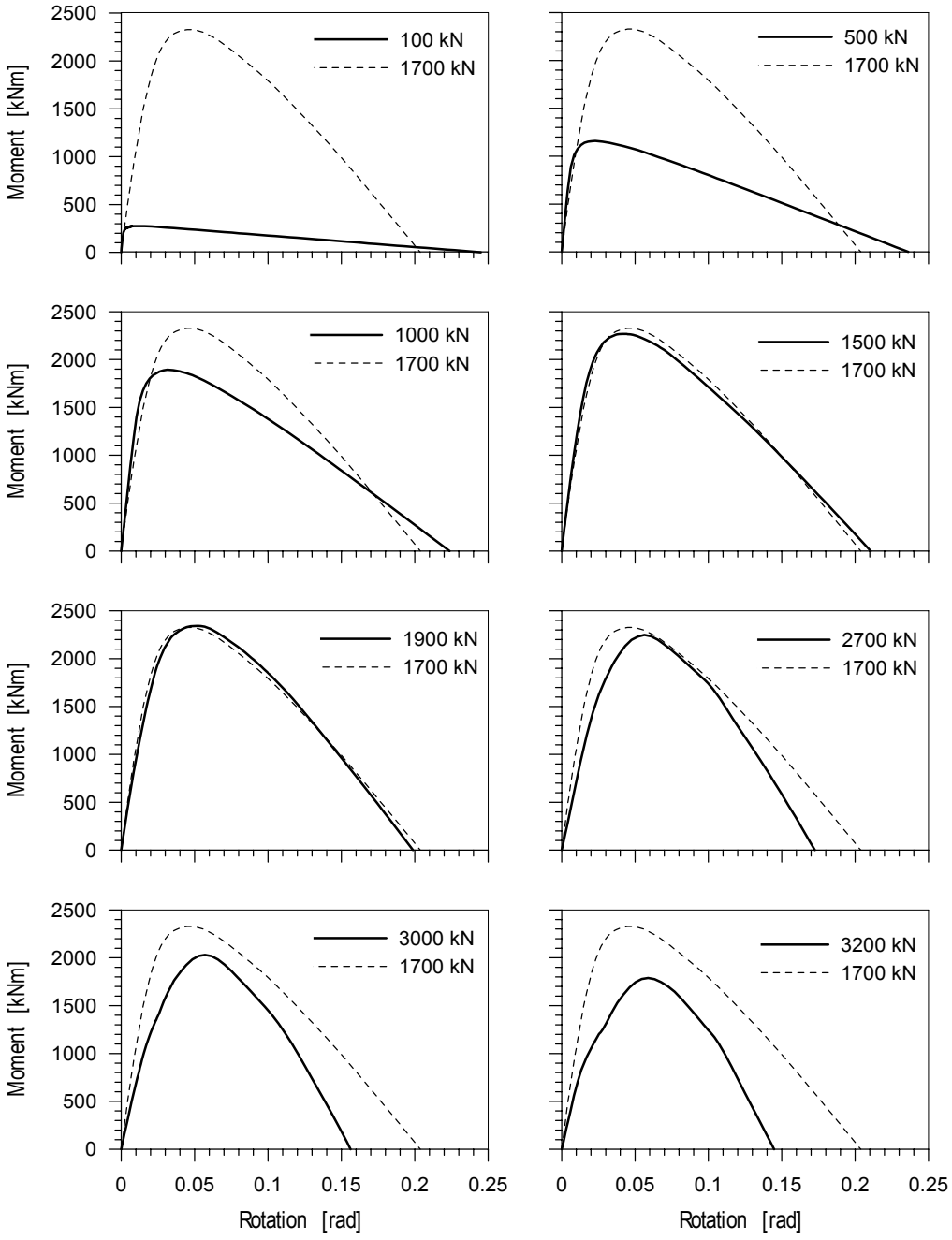

Figure 12 Moment–rotation curves for different values of axial load N

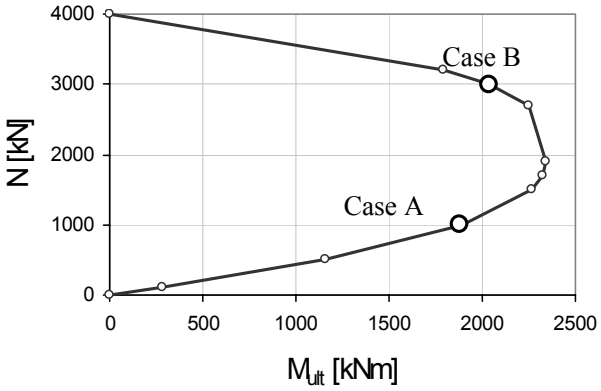

Figure 13 Failure locus of the interaction between vertical and moment loading for the footing of Figure 10, under a displacement-controlled horizontal forcing at the mass center of the superstructure

We focus now our attention to *Case B* where the central vertical load is three times as large as in *Case A* : $N = 3000 = 0.75N_{ult}$, i.e. a heavily loaded foundation (*F.S.* against bearing capacity failure ≈ 1.33). The moment capacity of the foundation is $M_{ult} \cong 2000$ kNm which approximates the *Case A* value. However, considerable soil yielding is now taking place even for low amplitudes of rocking prior to the onset of uplift, resulting to a softer $M–\theta$ curve (see Fig 12). Moreover, the extensive plastic deformation of the soil underlying the heavily loaded foundation, amplify the $P - \delta$ effects of the declining region and result to a more 'steep' M-θ curve. Eventually the moment becomes zero (that means pseudostatic overturning) for an angle of rotation $\theta = 0.16$ rad, whereas for the lightly loaded foundation the corresponding angle equals to 0.22 rad.

In Fig 14 the moment-vertical displacement curves are also plotted for both cases. In *Case A* the footing undergoes some small additional settlement during lateral loading until uplifting initiates. From this point on, it tends to move upwards leading to a positive displacement of the base center. In contrast, in *Case B* where uplifting is limited to a small portion of the base, dynamic settlement is significant and is gradually increasing during lateral loading. Eventually, at the time the overturning moment becomes zero due to P–δ effects, the downward displacement of the base center has come up to more than three times the static value. This tendency of the heavily loaded structure to respond by moving into the vertical direction as reflected by the high values of z_c, overshadows the uplifting potential of the foundation, up to quite high values of rotation preserving a full (or nearly full) contact condition for the soil-foundation interface.

Response under Seismic Loading

A long-duration Ricker pulse ($T_E = 2.2$ s, $PGA = 0.2$ g) is applied in the bedrock and is propagated through the soil to produce a free–field "input–motion" of a dominant period $T_E = 1.8$ s and $PGA = 0.32$ g as depicted in Fig 15. This long–duration type of motion resembles pseudostatically induced loading, so that the results would be comparable to those of the monotonic loading.

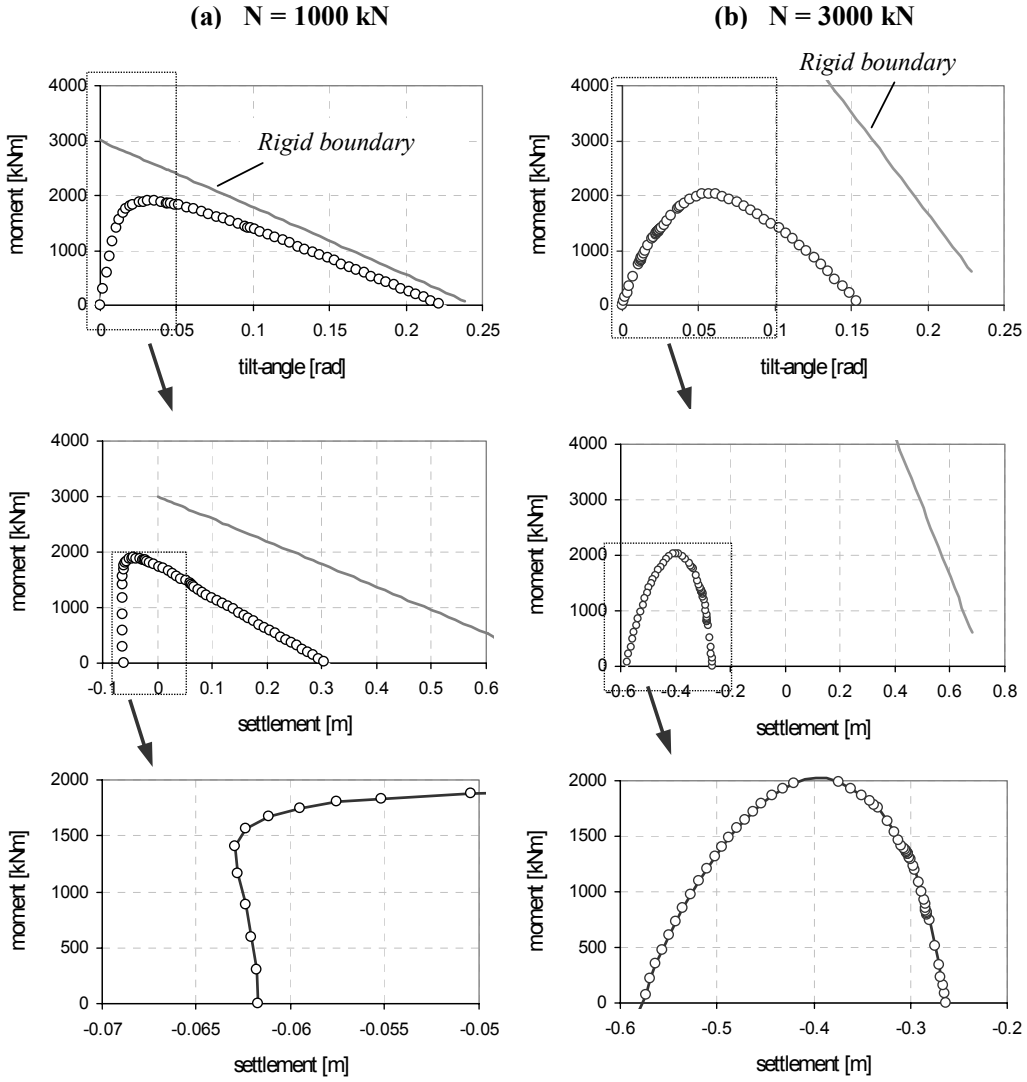

Figure 14 Load-deformation curves for the two loading cases under horizontal, monotonically increasing loading. The gray line corresponds to non-deformable soil

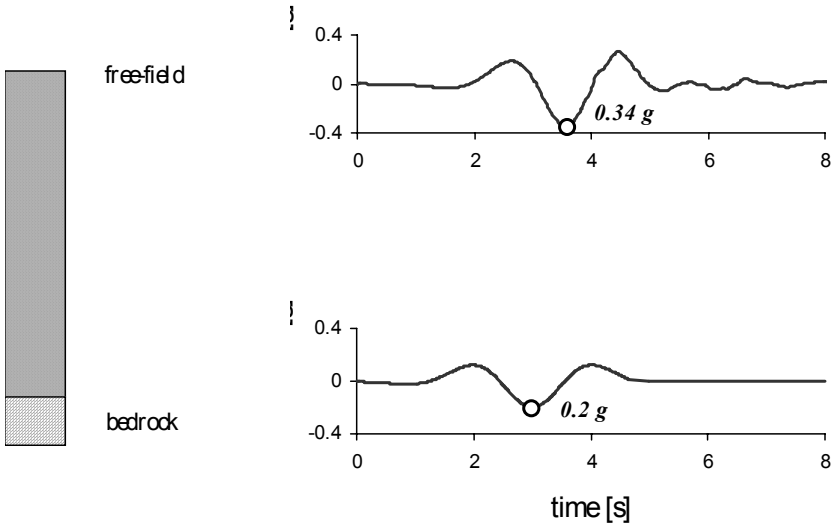

Figure 15 Soil amplification of the Ricker pulse-type motion

The load–deformation relationship for the two loading cases in terms of M–θ and M–z_c curves are plotted in Fig 16. The left-hand side figures refer to *Case A*, i.e. axial load N = 1000 kN or ¼ N_{ult}, and the right-hand side to *Case B*, i.e. axial load N = 3000 kN or ¾ N_{ult}. Several important conclusions can be drawn from these figures:

(a) Regarding the M–θ curves of *Case A*, the lightly loaded foundation (F.S. = 4): The initial loading cycle follows the monotonic static M–θ curve. Upon unloading after a small excursion in the descending branch of the monotonic curve, the path follows with small deviations the original monotonic curve. This is evidence of reversible behavior – indeed the result of nonlinearly elastic, uplifting response. However, after a substantial excursion into the descending branch, unloading departs slightly from the virgin curve, as soil inelasticity is "activated" due to the large concentration of the applied normal stress when uplifting reduces substantially the area of contact.

(b) Regarding the M–θ curves of *Case B*, the heavily loaded foundation (F.S. = 1.33): The departure of all branches of loading–unloading–reloading cycles from the monotonic curve is far more substantial – apparently the result of strongly inelastic soil behavior. Indeed the bearing capacity failure mechanisms are fully "activated" in this case.

(c) The moment-settlement curves (M–z_c) echo the above M–θ response, with the curve of *Case A* showing the smallest deviation from the monotonic curve, and of *Case B* the largest.

Time histories of the response for the (rigid) structure of *Case A* with the hypothetical case where the foundation is perfectly bonded to the inelastic soil and hence no uplifting occurs, are plotted in Fig 17. We notice that whereas the uplifting system experiences stronger oscillatory motion in terms of angle of rotation and vertical upward displacement, it enjoys smaller levels of acceleration. The latter is cut-off at the threshold acceleration defined by the moment capacity of the foundation:

$$M = N\,(a\,/\mathrm{g})\,h_{cm} \cong 0.16\ \mathrm{g}.$$

6. CONCLUSIONS

(a) The monotonic behavior of an uplifting foundation of a relatively tall structure is affected by: (i) the P–Δ phenomenon , (ii) the flexibility of the soil, and (iii) the magnitude of the normal force compared with the vertical bearing capacity of the foundation (i.e., the static factor of safety).

(b) Under seismic loading, toppling might not occur even when the instantaneous factor of safety against overturning (with bearing capacity exceedance) is well below unity. The nature of seismic excitation (specifically its frequency composition and, especially, the presence of a sequence of long duration impulsive cycles) is the controlling factor of the response of a specific system.

(c) The initiation of uplifting and the mobilization of bearing capacity "failure" can be quite beneficial for the superstructure, under certain conditions related with the fundamental period of the structure and characteristics of ground shaking.

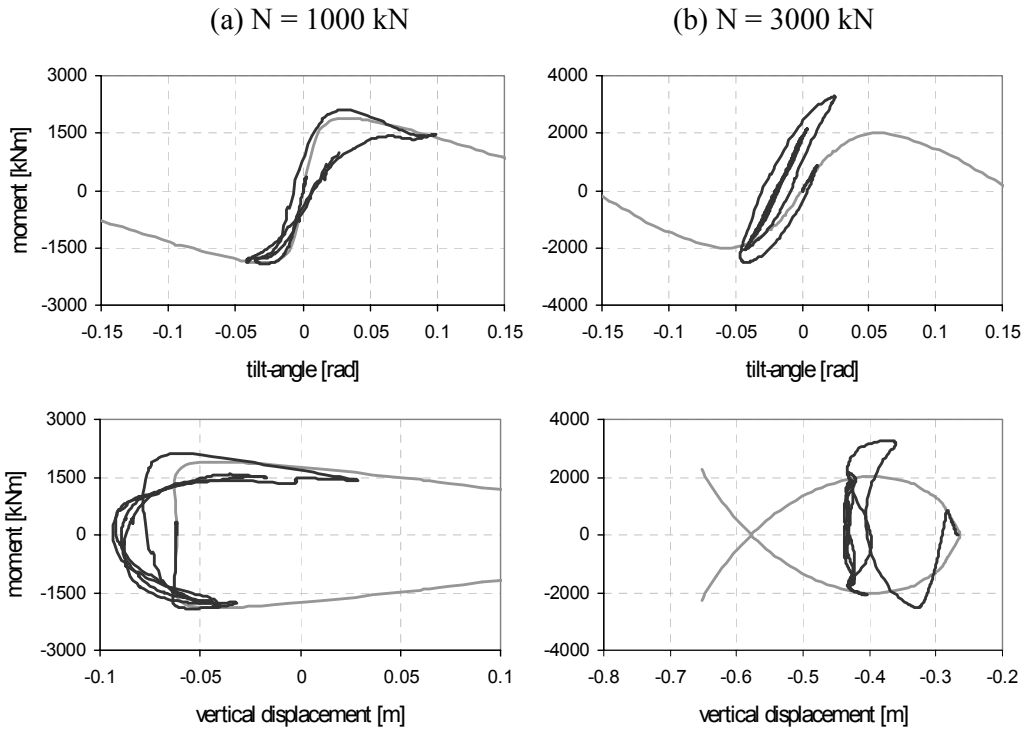

Figure 16 Load–deformation curves ($M–\theta$, $M–z_c$) for the two loading cases under earthquake loading. The outcropping excitation is a long duration Ricker pulse (PGA = 0.2 g, T_E = 2.2 s). The gray lines are the monotonic loading (plu s or minus) curves

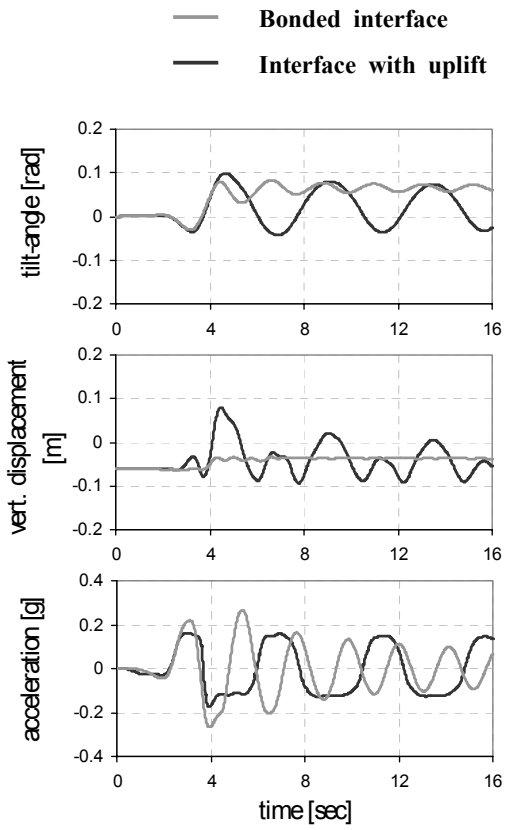

Figure 17 Time histories of the response for the case A, in conjunction with the system where soil can undergo tensile forces

7. REFERENCES

Allotey N, Naggar M., "Analytical moment-rotation curves for rigid foundations based on a Winkler model", *Soil Dynamics and Earthquake Engineering* 23 (2003) 367-381, 2003.

Apostolou M., Gazetas G., Makris N., Anastasopoulos J. "Rocking of Foundations under Strong Seismic Excitation". *Fib-Symposium on Concrete Structures in Seismic Regions*, Athens, 2003.

Bartlett P. "Foundation rocking on a clay soil" *ME Thesis,* University of Auckland, 1979.

Bransby M.F., & Randolph M.F., "Combined Loading of Skirted Foundations". *Geotechnique,* Vol. 48, pp. 637–655, 1998

Butterfield R. & Gottardi G., "A Complete Three Dimensional Failure Enveleope for Shallow Footings on Sand". *Geotechnique,* Vol. 44, pp. 181–184, 1994

Chopra A., Yim S. "Simplified Earthquake Analysis of Structures with Foundation Uplift". *Journal of Structural Engineering*, Vol. 114, No 4, 1985.

Cremer C., Pecker A., Davenne L. “Modeling of Nonlinear Dynamic Behaviour of a Shallow Strip Foundation with Macro-Element”. *Journal of Earthquake Engineering*, Vol. 6, No 2, 2002.

Earthquake Engineering Research Institute. “1999 Kocaeli, Turkey”. *Earthquake Reconnaissance Report*, Special Issue of Earthquake Spectra, 2001.

Gazetas G. “Foundation Failures in Adapazari during the 17–8–99 Izmit (Kocaeli) Earthquake”. *Proceedings of the 4th National Greek Conference on Geotechnical Engineering*, Athens, Vol. 3, 2001 (*in Greek*).

Gazetas G, Apostolou M., & Anastasopoulos I.X. “Seiemic Uplifting of Foundations on Soft Soil, with Examplesfrom Adapazari”. *Foundations: Innovations, Observations, Design, and Practice,* British Geotechnical Association, Thomas Telford, pp 37–50, 2003.

Hibbitt, Kalsson, and Sorensen. *Abaqus* v6.1, Rhode Island, 2001.

Japan Society of Civil Engineers . “The 1999 Kocaeli Earthquake, Turkey – Investigation into the damage to civil engineering structures”. *Report of Earthquake Engineering Committee,* 1999

Koh A., Spanos P., Roesset J. “Harmonic Rocking of Rigid Block on Flexible Foundation”. *Journal of Engineering Mechanics*, Vol. 112, No 11, 1986.

Pecker A., “Analytical Formulae for the Seismic Bearing Capacity of Shallow Strip Foundations”. *Seismic Behavior of Ground and Geotechnical Structures,* P. S. Seco e Pinto, Ed., A. A. Balkema, pp. 261–268, 1997

Poulos H.G., Carter J.P., Small J.C., “Foundations and Retaining Structures–Research and Practice”. Proceedings of the *15th International Conference on Soil Mechanics and Geotechnical Engineering,* Vol. 4, pp.2527–2605, Istanbul 2001.

Taiebat H.A. & Carter J.P. , “Numerical Studies of the Bearing Capacity of Shallow Foundations on Cohesive Soil Subjected to Combined Loading”. *Geotechnique,* Vol 50, pp409–418, 2000.

Psycharis I. “Dynamic Behaviour of Rocking Structures Allowed to Uplift”. *Journal of Earthquake Engineering and Structural Dynamics*, No 11, 1983.

.